

Crystalline Structure of Poly(ethylene terephthalate) Filaments

M. Youssefi,¹ M. Morshed,¹ M. H. Kish²

¹Department of Textile Engineering, Isfahan University of Technology, Isfahan 84156-83111, Iran

²Department of Textile Engineering, Amirkabir University of Technology, 15875-4413 Tehran, Iran

Received 21 November 2006; accepted 21 May 2007

DOI 10.1002/app.26806

Published online 1 August 2007 in Wiley InterScience (www.interscience.wiley.com).

ABSTRACT: Fully oriented, partially oriented, drawn, and quenched samples of poly (ethylene terephthalate) (PET) filaments were examined. Crystalline fraction and the average size of crystallites were measured by a wide angle X-ray scattering diffractometer. Sample geometry in X-ray diffraction was found to affect the intensity of the diffraction patterns. The crystalline fraction of the samples can be measured by X-ray diffraction in a symmetrical reflection geometry accompanied with curve fitting computer software. Annealing improves the average size of crystallites in a direction perpendicular to (010) plane more than the two other directions, namely perpendicular to (100) and (-105) planes. Fourier transform infrared spectroscopy was used to determine the percentage of trans configuration, and the

volume crystalline fraction was determined from density measurements. A good correlation was obtained between the percentage of trans configuration and weight percentage of crystalline fraction determined by density measurements. The molecular orientation of the samples was measured by a polarizing microscope and its results conform to the other findings. The presence of extended chains in the noncrystalline regions supports the idea of the presence of oriented amorphous (amorphous with correlation) and nonoriented amorphous domains in PET drawn filaments. © 2007 Wiley Periodicals, Inc. *J Appl Polym Sci* 106: 2703–2709, 2007

Key words: poly(ethylene terephthalate) (PET); structure; crystal structures; WAXS

INTRODUCTION

Considerable attempt has been made in the last few decades to describe the structure and properties of fibers, and for the sake of brevity a few are mentioned here.^{1–5} Several structural parameters such as crystalline fraction, molecular orientation index and so on have been defined. Different techniques have been used to determine these parameters. Among these techniques wide angle X-ray scattering (WAXS) provides basic information about the crystalline structure.¹ Molecular conformation can be deduced from infrared spectroscopy,⁶ molecular orientation can be determined from birefringence measurement,⁷ and the compactness of the structure can be evaluated from the density of fibers that may have different thermal and mechanical history.²

The presence of both sharp and diffuse diffraction effects in X-ray patterns of polymers have been accepted as evidence for a two-phase concept of polymer structure.¹ This means that relatively perfect crystalline domains are dispersed in amorphous regions.¹ However, there are disagreements between different investigators. For example Rastogi et al.,³ on the basis of several references, concluded that two

phase models are not adequate to describe properties such as oxygen permeability, mechanical behavior, heat capacity, and complex melting behavior of crystalline polymers. For poly (ethylene terephthalate) (PET) the amorphous phase has been shown to consist of two fractions. These fractions are the true or mobile amorphous fraction and the rigid amorphous fraction, which is partially ordered and is positioned between the mobile amorphous fraction and the crystalline region.³ Provorsek et al.⁴ have proposed a three-phase model for PET and polyamide fibers. These phases are oriented amorphous, nonoriented amorphous, and crystalline regions. Similar ideas have also been expressed by other authors.⁵ However, Abhiraman and coworkers⁸ stated that because of the simplicity of two-phase models and the absence of any objective framework for correlating with measures of order with three or more phase compositions, the two-phase model can be used and the inherent limitations should be taken in to account.

It is believed that the degree of crystalline fraction of a polymer is a concept that cannot be unambiguously defined.¹ Numerical values of crystalline contents obtained by X-ray techniques should be considered as an index of crystalline fraction and it should not be considered as an absolute measure.¹

Hermans and Weidinger⁹ determined the crystalline fraction from the ratio of the integrated intensity under the crystalline peaks to the integrated

Correspondence to: M. Morshed (morshed@cc.iut.ac.ir).

intensity under the complete diffraction trace. There was a difficulty in separating the crystalline peaks from the amorphous background. Several investigators tried to overcome this difficulty.^{10–13} Farrow and Peterson¹¹ used the amorphous pattern of PET yarns as a template. Dumbleton and Bowles¹² used an equation in the form of $C = 1 - (A/A_{100})$ to determine the crystalline fraction (C), where A is the ratio of intensities of 14° and 28.5° for any given sample and A_{100} is the value of this ratio for the quenched amorphous sample.

For measuring relative crystalline fraction a method called correlation crystallinity index is used by many authors¹⁰ The method is based on the relative classification of the equatorial trace of a partly crystalline sample between the traces of two standard samples ranked with zero and 100% crystallinity. The method of Hindeleh and Johnson¹⁰ is based on the resolution of normalized diffraction peaks in terms of combined Gaussian–Cauchy profiles for each peak, together with a polynomial background. Peak area crystallinity is then measured as the total area under the resolved peaks over a defined range.

The crystalline system of PET is known to be triclinic^{1,14}; the crystalline c axis is very close to the direction parallel to the fiber axes. It does not present (hkl) planes normal to the c axis with observable intensity.¹⁵ However, the planes with Miller indices $(-1\ 0\ 5)$ give a very strong X-ray diffraction intensity and their normal makes an angle of 9.77° with the c axis, calculated with the PET lattice parameters given by Daubney et al.¹⁴ The $(-1\ 0\ 5)$ reflection is used for the evaluation of crystalline orientation factor (f_c). Often it does not overlap with other (hkl) reflections.¹⁵ Dumbleton and Bowles¹² used the azimuthal scan of X-ray diffraction intensity distribution from $(-1\ 0\ 5)$ planes to calculate f_c .

In the chain axis direction of PET, there are some difficulties to measure the crystallite sizes accurately. The Scherrer equation is commonly used to calculate the crystallite sizes. The precision of crystallite size analysis using this equation is in the order of $\pm 10\%$.¹⁶ It is well known that postdraw heat treatments cause appreciable crystal growth, especially at temperatures exceeding 200°C .²

In spite of vast number of studies that have been conducted on the structure of PET fibers, it seems that more investigations are needed to reveal more details. The purpose of this article is to study the crystalline structure and morphology of some PET fibers with different microstructures. Different methods such as WAXS, Fourier transform infrared spectroscopy (FTIR), birefringence, and density measurements have been used. The WAXS experiments were made in symmetrical reflection geometry. In Ref. 1 a comprehensive description of different geometries of diffraction has been given. According to Alexander,¹

polymer patterns can be measured with X-ray counter diffractometer by means of one of the three geometrical arrangements: symmetrical reflection, normal beam transmission, and symmetrical transmission. Applying each of these techniques has its advantages and limitations; e.g. the intensities recorded by transmission will be much smaller than those measured by reflection since the parafocusing principle is utilized in the latter but not in the former technique. Besides, in the reflection technique the irradiated surface of the specimen must be planar and much care must be taken to obtain a flat surface, especially for Bragg angles smaller than 30° . The published literature examining the PET fibers in symmetrical reflection geometry are scarce but the instruments with this geometry are abundant. The $(-1\ 0\ 5)$ peak intensity was used to estimate the longitudinal crystallite size of the fibers.

EXPERIMENTAL

Partially oriented yarn (POY), 267 dtex, 48 filaments, and fully drawn yarn (FOY), 78 dtex, 34 filaments PET, both were supplied by Polyacril Company, Isfahan, Iran; these yarns contained 0.3% TiO_2 and were used as received. One amorphous sample was prepared by melting some filaments at 280°C in a sealed capsule and cooling rapidly in ice water. POYs were drawn in a single heater drawing machine at 80°C . The specifications of samples are summarized in Table I.

The X-ray diffraction patterns of the samples were obtained by using a Philips X-ray diffractometer model Xpert MPD with symmetrical reflection geometry. The Cu K_α radiation generated at 40 KV and 30 mA was used. The scattering intensities were recorded every 0.05° in the range of $2\theta = 10\text{--}50^\circ$. Time per step was 10 s.

Samples were prepared in two different forms. In the first form, the filaments were horizontal and used for equatorial scan. The parallel bundles of filaments were prepared by winding the yarns around a $1\text{ cm} \times 1\text{ cm}$ frame. These samples were mounted

TABLE I
Specifications of the Samples

Sample	Specification
AM	Quick quenched sample obtained by melting the fibers in a sealed capsule at 280°C and cooling rapidly in ice water
POY	Partially oriented yarn
FOY	Fully oriented yarn
DR1.8	The POY yarn was drawn in a drawing machine at 80°C with the draw ratio of 1.8
AN	Sample DR1.8 was annealed in a vacuum oven at 240°C for 24 h

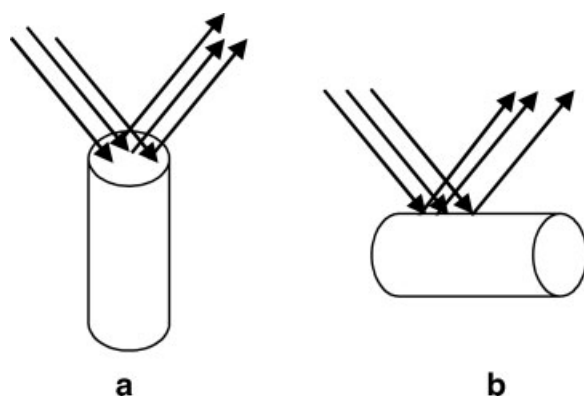


Figure 1 Schematic diagram of (a) vertically positioned fibers (meridional scan) and (b) horizontally positioned fibers (equatorial scan) in WAXS instrument (symmetrical reflection geometry). The arrows show the direction of incident and reflected X-ray beams.

horizontally in the sample holder of WAXS instrument and direction of incident beam was perpendicular to the fibers axis. In the second form, the filaments were vertical and used for meridional scan. The filaments were paralleled and then the ends were glued. The bundle of filaments was mounted vertically in the sample holder and the superfluous fibers were cut. In both cases, care has been taken to have a flat surface with suitable thickness.¹ Figure 1 shows the X-ray direction with respect to the fiber geometry for vertically positioned fibers (meridional scan) and for horizontally positioned fibers (equatorial scan) in WAXS instrument.

The WAXS patterns are analyzed by curve-fitting procedures to separate crystalline reflections from amorphous scattering to obtain crystallinity and crystallite sizes. The separation of amorphous and crystalline contributions in diffraction patterns is a necessary step in the study of crystallinity of semi-crystalline polymers.¹ For this purpose, we used commercial software PEAKFITTM.¹⁷ In the equatorial

scans, first a straight line was drawn in the diffractogram from $2\theta = 10^\circ$ to $2\theta = 35^\circ$ and the area under the line was subtracted from the background of the curve. Then four initial peaks were set, three of them for crystalline reflections (peaks No. 1–3) and one for amorphous scattering (peak No. 4). No constraints were made for center and amplitude of the peaks. The peak shapes were modeled by a Pearson VII function. The method of least square was used for the minimization of the errors.

Lateral crystallite sizes were determined for the equatorial peaks at $2\theta = 17^\circ$ and $2\theta = 23^\circ$ ((010) and (100) reflections, respectively) and longitudinal crystallite size was estimated from the nearly meridional peak at $2\theta = 43^\circ$ ((-105) reflection). The Scherrer equation [eq. (1)] was used to compute the mean crystallite size.¹

$$l_{(hkl)} = \frac{k\lambda}{\Delta_{(hkl)} \cos \theta} \quad (1)$$

where $l_{(hkl)}$ is the mean dimension of crystallite size perpendicular to the planes (hkl) , Δ represents full width at half maximum intensity, k is taken equal to one, θ is the diffraction angle, and λ is the X-ray wavelength. Table II shows the indexes, intensities, and Bragg spacing of all the WAXS reflections of the samples, which were observed in both equatorial and meridional scans. Also average crystallite lengths of the samples in different directions are shown in Table IV.

The density gradient column was prepared using higher ($\rho = 1.5 \text{ g/cm}^3$) and lower ($\rho = 1.27 \text{ g/cm}^3$) density solutions of calcium nitrate in water. The column with a linear density gradient was maintained at a constant temperature (23°C) using a water jacket around it. The fibers were wetted out with the lower density solution before they were introduced into the column. The final reading of the location of fibers in the column was obtained 4 h

TABLE II
Specifications of the WAXS Reflections of the Samples

Sample	Reflections Index	Equatorial			Meridional -105
		010	110	100	
POY	Intensity (a.u)	288	478	469	1,018
	2θ (degrees)	16.025	22.025	25.025	43.625
	Bragg spacing (\AA)	5.53	4.04	3.56	2.07
DR1.8	Intensity (a.u)	1,267	238	4,333	2,339
	2θ (degrees)	17.525	22.025	25.325	43.325
	Bragg spacing (\AA)	5.06	4.04	3.52	2.09
FOY	Intensity (a.u)	4,418	2,886	9,670	11,350
	2θ (degrees)	17.525	22.925	25.625	43.025
	Bragg spacing (\AA)	5.06	3.88	3.48	2.10
AN	Intensity (a.u)	39,566	45,535	89,368	19,499
	2θ (degrees)	17.525	22.625	25.625	42.435
	Bragg spacing (\AA)	5.06	3.93	3.48	2.13

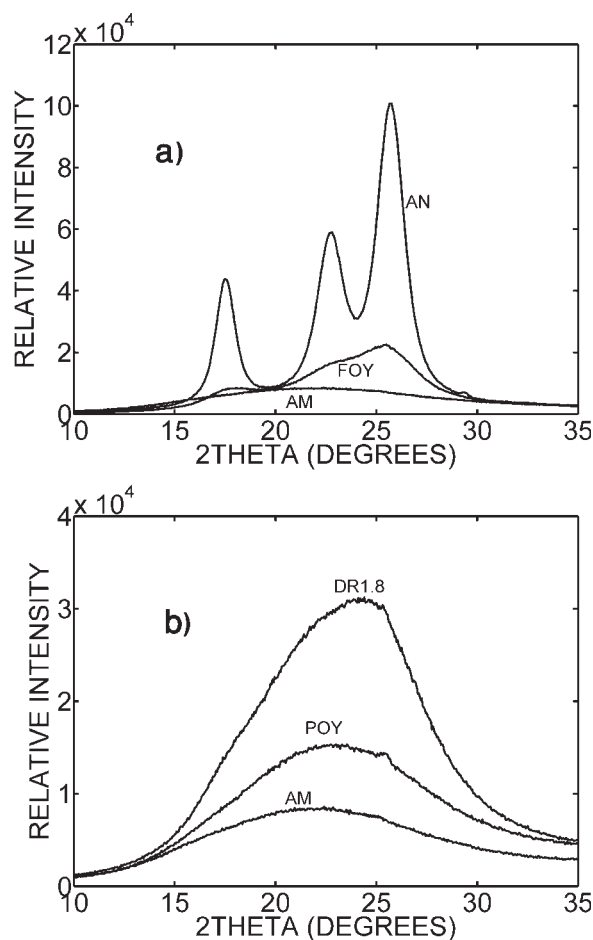


Figure 2 Equatorial WAXS scan of the samples (fibers were horizontally positioned).

after the introduction of the fibers. The values were not corrected for the TiO_2 content. Three specimens of each fiber sample were used for the measurements. The degree of crystallinity, expressed as a volume fraction (x), was obtained using [eq. (2)].

$$x = \frac{\rho - \rho_a}{\rho_c - \rho_a} \times 100 \quad (2)$$

Where ρ is the density of the fibers and ρ_c and ρ_a are densities of crystalline and amorphous phases, respectively. Different values for fully crystalline PET have been reported in the literature. Geil¹⁸ tabulated these values. The differences were because of the different unit cell dimensions. In this work, the value of 1.457 g/cm^3 was used for ρ_c that seems to be more common for fibers. Similarly, for amorphous PET several values are reported: 1.333 g/cm^3 ,^{14,19} 1.323 g/cm^3 ,¹⁴ and 1.336 g/cm^3 .²⁰ In this work the value of 1.336 g/cm^3 was used for ρ_a .²¹

FTIR measurements were made using a Bomem MB-100 spectrophotometer with the resolution of 4 cm^{-1} . The FTIR spectra were analyzed by fitting

Pearson IIV profiles to the absorption bands present over the range of $930\text{--}760 \text{ cm}^{-1}$ (Ref. 22) using Peak-fit™ software.¹⁷ The trans and gauche bands used for determination of rotameric compositions are 846 and 898 cm^{-1} , respectively.

Birefringence was measured using a Zeiss polarizing microscope equipped with a 30th order tilting compensator.

RESULTS AND DISCUSSION

Figure 2 shows equatorial WAXS scan of diffraction profiles of AN, POY, AM, and DR1.8 samples that were positioned horizontally. As shown in Figure 2 no sharp crystalline peaks can be seen in the X-ray diffraction patterns of different samples except for the AN sample. As expected, sample AN has the highest crystallinity because of the effect of annealing. Figure 3 shows the meridional WAXS scan of the samples, which was taken from fibers cross section (fibers were positioned vertically). In the meridional scans of FOY sample, a very sharp peak is observed at about $2\theta = 43^\circ$, which relates to $(-1\ 0\ 5)$ planes reflection and is not detectable with equatorial scans. This indicates that a remarkable crystalline fraction exists in this sample, even though no resolved peak is observed in the equatorial scan of this sample [Fig. 2(a)]. In DR1.8 and POY samples the intensity of this peak is much smaller than the corresponding peak for FOY sample.

Figure 4 shows the profile fitted to WAXS scan of FOY sample. As shown in this figure, the difference between the observed intensities and the calculated curve, represented by Δ , is not significant.

It seems that the diffraction scans can be separated into the crystalline peaks and the scattered background on a same basis. Salem² states that a limita-

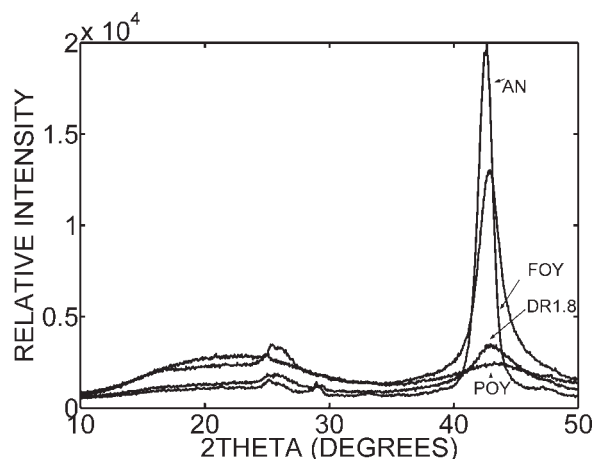


Figure 3 Meridional WAXS scan of the samples from fibers cross section (fibers were vertically positioned).

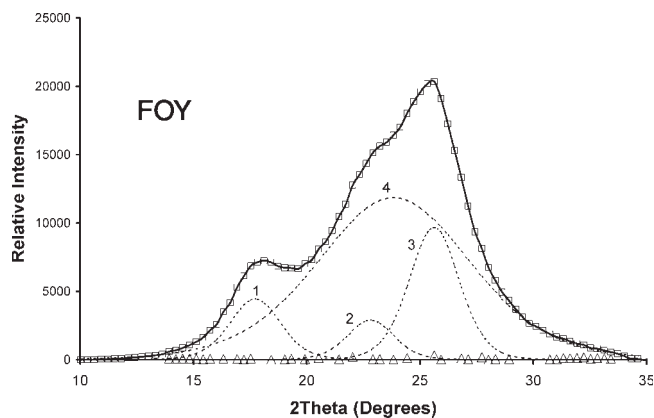


Figure 4 Profile fitted to WAXS scan of FOY sample. Dashed lines represent the resolved components (Peaks 1 through 4), full line represents the sum of resolved components (calculated curve), \square represents the observed data, and Δ represents the difference between the observed intensities and the calculated curve. The above resolving procedure was performed on AN, POY, and DR1.8 samples too.

tion of X-ray diffraction is that the presence of crystallinity cannot generally be detected when the volume fraction of crystallinity is less than about 10%, because at these crystallinity levels the crystalline reflections are so weak that they are submerged in scattering from the amorphous fraction. However, using this method, we were able to compare the relative crystallinity of the above mentioned samples. By X-ray diffraction method, as expected, the POY sample shows a very low crystallinity of about 2%. In DR1.8 samples the amount of crystalline fraction is about 7%.

According to Geil,¹⁸ ice-water quenching from the melt is not sufficient to produce wholly amorphous structureless samples and results in a domain structure that has an aligned nematic liquid-like packing of the chain samples. Also for the crystalline regions, he states that there are no universal unit cell parameters that can be said to be appropriate for all PET crystals prepared by different procedures. So it seems that the relative crystallinity, which is obtained by using eq. 2, must be considered as relative amounts.

Farrow and Ward²³ compared the crystallinity of PET fibers determined by methods based on density, infrared spectra, and X-ray diffraction and found no correlation between the results. They also stated that the values from infrared spectra are high, those from X-ray measurement are low, and those from the density fall roughly between the two. In the present work, the results of relative crystallinity measurements obtained from X-ray diffraction and density measurements show that X-ray crystallinity is lower than the crystalline fraction determined by density measurements. It is clear from these data that con-

siderable differences exist in the estimates of simple two-phase crystallinity by different methods. A common inference regarding differences between crystalline fractions obtained via bulk density and WAXS is that it is possibly a reflection of changes in the density of noncrystalline phase due to the molecular orientation. Sharma et al.⁸ did not find a good correlation between the estimated noncrystalline phase density and its birefringence. It seems that this phenomenon needs more investigations.

For the sample DR1.8, there is has even a larger difference in the estimated relative crystallinity by these two methods. This may be because of the higher amount of extended noncrystalline chains, which exist in the amorphous portion of this sample. It means that in drawing of the POY at few degrees above the glass transition temperature (80°C), many chains in the amorphous portion become extended and this causes an increase in density of this sample, and therefore the extent of relative crystallinity obtained by density method is much higher than that obtained by WAXS method.

A representative FTIR spectrum and its nonlinear squares best-fit curve for the regions of 750–950 cm^{-1} are displayed in Figure 5. The trans conformation is considered representative of extended chain segments, and the gauche conformation is the representative of the coiled or folded chain segments.²² The trans content or trans–gauche ratio gives the ratio of extended chain segments to the random coiled segments. To obtain the ratio of trans conformers, the intensity of the trans absorption at 848 cm^{-1} is divided by the sum of the intensities of the trans and the gauche bands (at 898 cm^{-1}).²²

Table III shows the percentage of trans configuration, density, and relative crystallinity of the samples. The percentage of trans increases with the increase of density and relative crystallinity of the

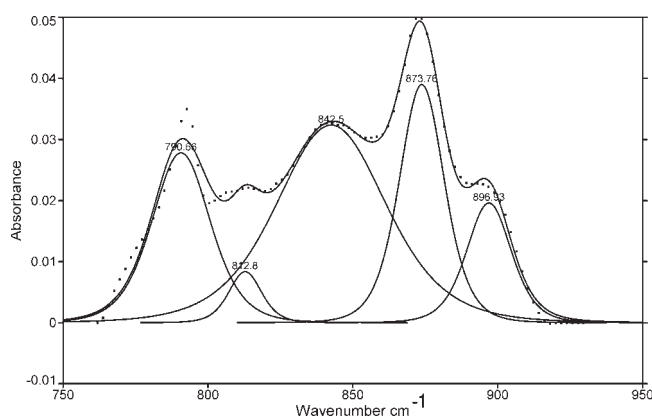


Figure 5 The FTIR spectrum of AM sample. Dots represent the observed data, full lines represent the resolved components and the sum of resolved components (calculated curve) ($r^2 = 0.99$).

samples. The correlation coefficient between percentage of the trans conformation and the relative crystallinity from density measurements was found to be $r^2 = 0.995$. This correlation coefficient is significantly higher than that of the trans percentage and relative crystallinity from WAXS, that is $r^2 = 0.895$. This result shows that there may be a comparatively higher amount of extended chains in noncrystalline regions, which causes more packing of the chains and therefore higher density for these regions.

As shown in Table IV, crystallite dimensions are in a direction perpendicular to the planes of (010), (100), and (-105). These three dimensions are designated by $\delta_{(010)}$, $\delta_{(100)}$, and $\delta_{(-105)}$ respectively. The crystallite sizes are in the range of what has been reported in the literature.² Average size of crystallites in AN samples in all directions are greater than those of other samples. This is because of annealing, which causes the growth of crystals. In the two low crystallinity samples (POY and DR1.8) the crystallite size must be regarded with more caution especially in the lateral directions. It is clear that a good correlation exists between the relative crystallinity and the longitudinal crystalline length of the samples. In other words, the longitudinal crystallite length in the chain direction is proportional to the relative crystallinity of the samples. The crystallite volume of the samples also has a good correlation with crystalline fractions.

Comparison of crystallite size of the AN and FOY samples shows that the growth of crystallites due to the thermal treatments on the direction perpendicular to (010) planes is greater than those for the directions perpendicular to (100) and (-105) planes. Huisman and Heuvel²⁴ examined the effects of temperature, tension, and duration of heat treatment on the physical structure of PET yarns using WAXS and density measurements and stated that the growth in the direction perpendicular to (010) plane is stronger than those of the other lateral directions. They interpreted this effect in terms of the reported different interactions between molecules of poly(ethylene terephthalate). It was found that the dipole-dipole interactions between adjacent ester groups, i.e. along the *b*-axis, are stronger than the interaction via the aromatic Π -electrons of the benzene groups. The

TABLE III
Percentage of Trans Configuration, Density, Birefringence, and Relative Crystallinity of the Samples

Sample	Density (g/cm ³)	%Trans	% Crystalline fraction		Birefringence
			Density	WAXS	
AM	1.336	73.4	—	—	—
POY	1.342	81.3	5.14	2.21	0.0479
DR1.8	1.380	89.8	35.44	6.60	0.1969
FOY	1.391	89.9	44.07	31.82	0.1964
AN	1.437	98.7	80.22	78.61	0.2124

TABLE IV
Crystallite Size of the Samples in Different Directions

Sample	$\delta_{(010)}$ (Å) ^a	$\delta_{(100)}$ (Å) ^b	$\delta_{(-105)}$ (Å) ^c	Crystallite volume (Å ³)
POY	19.7	47.2	15.5	14,412
DR1.8	35.2	29.2	23.1	23,473
FOY	33.8	34.8	45.7	53,754
AN	76.4	58.2	70.3	312,587

^a Crystallite size in the direction perpendicular to (010) planes.

^b Crystallite size in the direction perpendicular to (100) planes.

^c Crystallite size in the direction perpendicular to (-105) planes.

observed direction of the strongest growth is the one in which the intermolecular interaction between ester dipoles exists. So the system of crystallization of polymer prefers to reach to its minimum energy by preferred crystallization in the direction of the strongest interaction. This point will be more clear if we consider another thermoplastic polymer such as polyethylene (PE). According to Hikosaka et al.,²⁵ the mechanism of lamellar thickening growth of PE differs for the two directions of longitudinal and lateral. However, no difference between the growths of crystallites in different lateral directions was mentioned. So it seems that the existence of the benzene ring in PET could be responsible for different growth rate in different lateral directions.

Gupta and Kumar²⁶ reported an increase in the crystallite size of PET fibers due to heat setting and stated that the results for crystallite size from (100) plane show similar trends to those for the (010) plane. Fu et al.²⁷ stated that annealing causes the crystallites in PET fibers to grow in all directions. They also stated that applying tension during annealing causes the crystallites to grow preferentially along the direction of the applied force, but the volume of the crystallites does not increase significantly with the application of force. In a recently published elaborated article, Murthy and Grubb²⁸ stated that small size crystallites imply a larger surface area and more interdomain linkages. These linkages appear to be the key in the polymer stiffness.

The results of birefringence measurements of the samples shown in Table III indicate that there is a noticeable difference in molecular orientation among these samples. Two samples of FOY and DR1.8, in spite of having different structures, show almost the same total molecular orientation.

CONCLUSIONS

From the results of different experiments on the different PET fibers in this study, the following conclusions may be drawn:

1. It seems that two-phase models can be used as a practical model to determine the relative crystalline fractions of the samples. However, as it is previously found by a number of authors, the percentage of crystalline fractions obtained by these methods are not absolute and should be regarded as an index for relative comparisons. Further details of structure can be possibly obtained by more powerful, sensitive, and adaptable instruments.
2. Density measurements, infrared spectroscopy, birefringence, and X-ray diffraction studies measure different aspects of PET fiber structure and from these data it is inferred that there are some differences in the amorphous structure of different samples. In other words, the division of amorphous regions to "amorphous with correlation" and "wholly amorphous" by Morton and Hearle⁵ is supported.
3. It seems that in WAXS the meridional scan of the fibers in the symmetrical reflection geometry can be obtained by subjecting the cross section of a bundle of fibers to X-ray beam. By this method it will be possible to measure the longitudinal size of crystallite.
4. Comparison of crystallite size of the samples in different directions shows that the crystallite size growth of PET fibers due to thermal treatments differs in different lateral and longitudinal directions.
5. Density measurement is more sensitive to little differences for the samples with low crystalline fraction than WAXS measurements.
6. There are some more structural parameters that can not be easily determined by the present state of the equipments, and further work is required to determine the absolute values of structural parameters of PET filaments.

References

1. Alexander, L. E. X-ray Diffraction Methods in Polymer Science; Wiley-Interscience: New York, 1969; p 137.
2. Salem, D. R. In Structure Formation in Polymeric Fibers; Salem, D. R., Ed.; Hanser Publishers: Munich, 2000; p 493.
3. Rastogi, R.; Welinga, W. P.; Rastogi, S.; Schick, C.; Meijer, H. E. H. *J Polym Sci B*, 2004, 42, 2092.
4. Provorsek, D. C.; Tirpak, G. A.; Harget, P. J.; Reimamschuessel, A. C. *J Macromol Sci Phys* 1974, 9, 733.
5. Morton, W. E.; Hearle, J. W. S. Physical Properties of Textile Fibers, 2nd ed.; Textile Institute: Manchester, 1986; p 35.
6. Boerio, F. J.; Bahl, K. *J Polym Sci Polym Phys Ed* 1976, 14, 1029.
7. H.de Veris, J. *J Polym Sci* 1959, 34, 761.
8. Sharma, V.; Desai, P.; Abhiraman, A. S. *J Appl Polym Sci* 1995, 65, 2603.
9. Hermans, P. H.; Weidinger, A. *Text Res J* 1961, 31, 558.
10. Hindeleh, A. M.; Johnson, D. J. *Polymer* 1978, 19, 27.
11. Farrow, G.; Peterson, D. *Br J Appl Phys* 1960, 11, 353.
12. Dumbleton, J. H.; Bowles, B. B. *J Polym Sci A-2* 1966, 4, 951.
13. Farrow, G. *Polymer* 1960, 1, 518.
14. Daubney, R. P.; Bunn, C. W.; Brown, C. J. *Proc R Soc London* 1954, 226, 531.
15. Auriemma, F.; Guerra, G.; Parravicini, L.; Petraccone, V. *J Polym Sci B* 1995, 33, 1917.
16. Azaroff, L. V. *Elements of X-Ray Crystallography*, McGraw-Hill: New York, 1968; p 552.
17. <http://www.systat.com/products/PeakFit>.
18. Geil, P. H. In *Handbook of Thermoplastic Polyesters: Homopolymers, Copolymers, Blends and Composites*, Vol. 1; Fakirov, S., Ed.; Wiley-VCH: Weinheim, 2002; p 105.
19. Fischer, E. W.; Fakirov, S. *J Mater Sci* 1976, 11, 1041.
20. Wunderlich, B. *Thermal Analysis of Polymeric Materials*; Springer: Berlin, 2005.
21. Bourvellec, G. L.; Beautemps, J. *J Appl Polym Sci* 1990, 39, 329.
22. Roland, C. M.; Sonnenschein, M. F. *Polym Eng Sci* 1991, 31, 1434.
23. Farrow, G.; Ward, I. M. *Polymer* 1960, 1, 330.
24. Huisman, R.; Heuvel, H. M. *J Appl Polym Sci* 1978, 22, 943.
25. Hikosaka, M.; Amano, K.; Rastogi, S.; Keller, A. *J Mater Sci* 2000, 35, 5157.
26. Gupta, V. B.; Kumar, S. *J Appl Polym Sci* 1981, 26, 1865.
27. Fu, Y.; Busing, W. R.; Jin, Y.; Affholter, K. A.; Wunderlich, B. *Macromolecules* 1993, 26, 2187.
28. Murthy, N. S.; Grubb, D. T. *J Polym Sci B* 2003, 41, 1538.